

SYMPOSIUM ON MICROGRAVITY FLUID MECHANICS

presented at

THE WINTER ANNUAL MEETING OF
THE AMERICAN SOCIETY OF MECHANICAL ENGINEERS
ANAHEIM, CALIFORNIA
DECEMBER 7-12, 1986

sponsored by

THE FLUIDS ENGINEERING DIVISION,
THE AEROSPACE DIVISION, AND
THE BIOENGINEERING DIVISION, ASME

edited by

D. J. NORTON
HOUSTON AREA RESEARCH CENTER

**PROPELLANT TANK FORCES RESULTING
FROM FLUID MOTION IN A LOW-GRAVITY FIELD**

J. Navickas¹, C. R. Cross², D. D. Van Winkle³
McDonnell Douglas Astronautics Company
Huntington Beach, California

ABSTRACT

An accurate prediction of forces exerted by propellant motion on the storage container is required for many space vehicles under a wide range of dynamic environments. Most approximate methods fail altogether or give overly conservative results. A finite difference technique to solve the equations of motion offers a substantial improvement over the approximate methods. One such program, HYDR-3D, developed by Flow Science, Inc., was chosen to conduct propellant motion analysis under some typical space dynamic environments. A partially filled spherical tank was subjected to rotational motion about an axis of rotation outside of the tank to determine the tank sidewall forces and moments caused by such a maneuver. The same tank was subjected to accelerations parallel to the tank axis in order to determine the acceptable acceleration levels to settle the propellant before the engine restart. The program was able to track the propellant configuration through large displacements and provide useful design data. Computed results also compared well with cylindrical container test data at a relatively low Bond number with large liquid surface deformations.

NOMENCLATURE

A	=	fractional area open to flow
a	=	acceleration
b	=	loss across a porous baffle
F	=	volume fraction occupied by fluid
f	=	viscous acceleration
p	=	pressure
t	=	time
u	=	x-velocity
V	=	fractional volume open to flow
v	=	y-velocity z-velocity
wsx	=	wall shear stress
wsy	=	wall shear stress
wsz	=	wall shear stress
x	=	coordinate axis
y	=	coordinate axis
z	=	coordinate axis
μ	=	viscosity
ρ	=	density
τ	=	shear stress

Subscripts

r	=	radial
x	=	x-direction
y	=	y-direction
z	=	z-direction

INTRODUCTION

Propellant response to dynamic excitations in a low-gravity field has always been an area of concern in the design of space systems. These concerns are amplified as the performance requirements for many space-operating systems become quite demanding. Since many vehicles are launched from the Shuttle payload bay, forces and moments applied to the vehicle during the ejection stage must be determined to evaluate clearance and vehicle control requirements. The unbalanced moments are caused by an unsymmetric propellant configuration, where the liquid-vapor interface can assume a minimum energy configuration and be located anywhere in the tank before vehicle ejection from the payload bay. As the mission progresses, it is frequently necessary to position the propellant at a particular location within the tank for engine restart or other purposes. Therefore, the optimum acceleration levels and durations to accomplish this task with a minimum of vehicle and propellant disturbances have to be determined. Forces and moments during such settling maneuvers must be determined in order to establish the vehicle control requirements. Additionally, if a stable platform must be maintained after a vehicle maneuver, the force and moment calculations must be continued after the maneuver is completed.

Many techniques have been developed to determine propellant dynamics in a low-gravity field. An equivalent pendulum method, described by Abramson (1), has been used extensively in control system analysis. However, this method is not applicable at very low gravity levels or at large liquid surface deformations. NASA has used a KC-135A aircraft flying a parabolic trajectory to provide approximately 30 sec of zero-g environment, to experimentally evaluate fluid response to dynamic disturbances. Orbital experiments provide excellent means to evaluate low-gravity fluid dynamic behavior. However, such experiments are expensive, require a long lead time and do not allow

¹Principal Engineer/Scientist
²Engineer Scientist/Specialist
(presently with Astronautics Technology Center)
³Manager

continuous changes as the system design evolves. Numerical techniques have been undergoing intense development for a number of years. It appears that a point has been reached in this development to permit propellant response characteristics to be calculated for rather general dynamic environments. The present analysis was conducted to predict liquid dynamic response to a number of possible dynamic disturbances of a spherical propellant tank and to give some insight into the capabilities and limitations of the HYDR-3D (2) code.

COMPUTATIONAL METHOD

The HYDR-3D code is a result of many years of development of numerical techniques started with the Marker-and-Cell Program (3). The initial program evolved into many variations, some rather general, some oriented towards a specific task. The SOLA-SURF Program (4) is a two-dimensional program that has been used extensively. It accommodates liquid surface configurations of limited slope, hence it cannot be used where excessive surface deformations are encountered. The SOLA-VOF Program (5) is a two-dimensional program that can accommodate multi-valued liquid surface configurations, including breaking surfaces. This program has also been used in a variety of applications.

The HYDR-3D program is a three-dimensional program that can accommodate extensive surface deformations, including separation of liquid volumes from the liquid bulk. General initial fluid surface configurations and container geometries are represented by analytical expressions. Both liquid and vapor can be treated as either compressible or incompressible media. Surface tension and viscosity are also included. General vehicle motions are entered through a special routine that relates motion of a separate mesh coordinate system to an inertial reference system. Motion of rotating and translating systems can, therefore, be readily represented.

A fully compressible continuity equation and the Navier-Stokes equations of motion are solved by the program. The Cartesian form of the equations, taken from Reference (2), follows.

The fully compressible continuity equation is:

$$\nabla \frac{\partial \rho}{\partial t} + \frac{\partial}{\partial x} (\rho u A_x) + \frac{\partial}{\partial y} (\rho v A_y) + \frac{\partial}{\partial z} (\rho w A_z) = 0$$

The equations of motion are:

$$\frac{\partial u}{\partial t} + \frac{1}{V} \left[u A_x \frac{\partial u}{\partial x} + v A_y \frac{\partial u}{\partial y} + w A_z \frac{\partial u}{\partial z} \right] = -\frac{1}{\rho} \frac{\partial p}{\partial x} + g_x + f_x - b_x$$

$$\frac{\partial v}{\partial t} + \frac{1}{V} \left[u A_x \frac{\partial v}{\partial x} + v A_y \frac{\partial v}{\partial y} + w A_z \frac{\partial v}{\partial z} \right] = -\frac{1}{\rho} \frac{\partial p}{\partial y} + g_y + f_y - b_y$$

$$\frac{\partial w}{\partial t} + \frac{1}{V} \left[u A_x \frac{\partial w}{\partial x} + v A_y \frac{\partial w}{\partial y} + w A_z \frac{\partial w}{\partial z} \right] = -\frac{1}{\rho} \frac{\partial p}{\partial z} + g_z + f_z - b_z$$

The viscous accelerations are:

$$\rho V f_x = w s x - \left\{ \frac{\partial}{\partial x} (A_x \tau_{xx}) + \frac{\partial}{\partial y} (A_y \tau_{xy}) + \frac{\partial}{\partial z} (A_z \tau_{xz}) \right\}$$

$$\rho V f_y = w s y - \left\{ \frac{\partial}{\partial x} (A_x \tau_{xy}) + \frac{\partial}{\partial y} (A_y \tau_{yy}) + \frac{\partial}{\partial z} (A_z \tau_{yz}) \right\}$$

$$\rho V f_z = w s z - \left\{ \frac{\partial}{\partial x} (A_x \tau_{xz}) + \frac{\partial}{\partial y} (A_y \tau_{yz}) + \frac{\partial}{\partial z} (A_z \tau_{zz}) \right\}$$

where

$$\tau_{xx} = -2\mu \left\{ \frac{\partial u}{\partial x} - \frac{1}{3} \left(\frac{\partial u}{\partial x} + \frac{\partial v}{\partial y} + \frac{\partial w}{\partial z} \right) \right\}$$

$$\tau_{yy} = -2\mu \left\{ \frac{\partial v}{\partial y} - \frac{1}{3} \left(\frac{\partial u}{\partial x} + \frac{\partial v}{\partial y} + \frac{\partial w}{\partial z} \right) \right\}$$

$$\tau_{zz} = -2\mu \left\{ \frac{\partial w}{\partial z} - \frac{1}{3} \left(\frac{\partial u}{\partial x} + \frac{\partial v}{\partial y} + \frac{\partial w}{\partial z} \right) \right\}$$

$$\tau_{xy} = -\mu \left\{ \frac{\partial v}{\partial x} + \frac{\partial u}{\partial y} \right\}$$

$$\tau_{xz} = -\mu \left\{ \frac{\partial u}{\partial z} + \frac{\partial w}{\partial x} \right\}$$

$$\tau_{yz} = -\mu \left\{ \frac{\partial v}{\partial z} + \frac{\partial w}{\partial y} \right\}$$

Fluid configurations are defined in terms of volume of fluid function. This function represents the volume of fluid 1 per unit volume and satisfies the equation

$$\frac{\partial F}{\partial t} + \frac{1}{V} \left[\frac{\partial}{\partial x} (F A_x u) + \frac{\partial}{\partial y} (F A_y v) + \frac{\partial}{\partial z} (F A_z w) \right] = 0$$

Either no-slip or free-slip boundary conditions can be input at solid boundaries. These conditions are imposed after each pass through the mesh during the pressure iteration.

Surface tension effects are input in an explicit fashion by adjusting the pressure component in the equations of motion.

The computational scheme normally employed is a modified donor-cell method which is first-order accurate in space and time. Although a second-order method is available as an option in the program, the first-order method is adequate for most solutions.

COMPUTATIONAL RESULTS

Limited comparisons of computed results to test data indicate that the program can predict fluid dynamic behavior under a wide range of conditions. The program has been used to calculate liquid surface displacement and liquid forces in a sinusoidally excited spherical tank (2). Results compare well to test data. However, the solution represents linear range with a well-behaved single-value liquid surface. Estes et al. (6) predicted with fair accuracy propellant-induced forces and moments in a KC-135 test using a predecessor of the HYDR-3D program. Torrey (7) used the SOLA-VOF program to compute low-gravity liquid settling including surface tension. Results compare well to test data, although the resolution of the test data is rather limited, since liquid configuration in a drop tower test was obtained from a movie film. In the experiment, acceleration was applied to settle liquid from the top to the bottom of a cylindrical tube with hemispherical

ends. The Bond number was calculated to be 4.1, indicating that surface tension forces play a significant role. Large surface deformations are also present. Such a case is rather demanding on the computational method. This problem was solved using the HYDR-3D program with a 7×30 grid. Torrey (7) used a 12×40 node grid in his analysis. The number of nodes represents one half of the test container, due to the cylindrical symmetry. The test cylinder is 4 cm in diameter and 9 cm long. The test fluid, ethanol, has the following properties: density, 0.789 g/cm^3 ; surface tension coefficient, 22.33 dynes/cm ; kinematic viscosity, $0.001095 \text{ cm}^2/\text{sec}$ and an applied settling acceleration of 29.0 cm/sec^2 . Using a computational time interval of 0.0001 sec , as compared to the minimum computational time interval of 0.0015 sec calculated by the automatic computational time-interval generator built into the program, improved the stability of the solution. A no-slip condition at the container sidewalls was assumed. A comparison of analytical results to test data at four time points is shown in Figure 1.

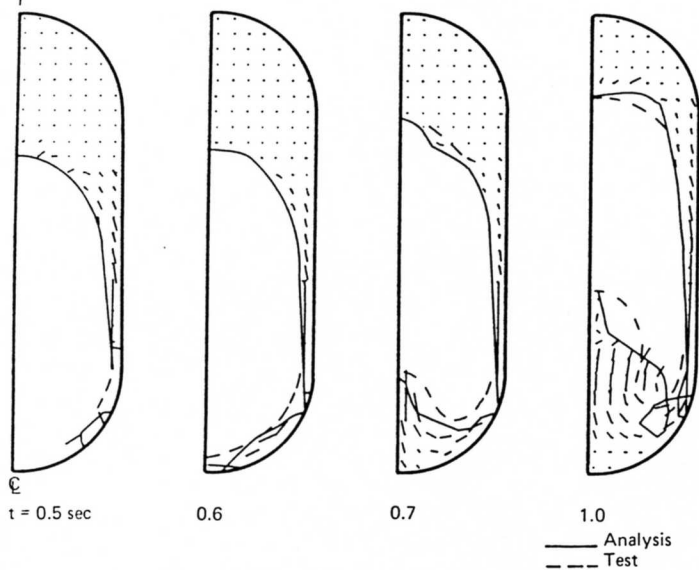


Figure 1. Liquid Surface Configuration

Fluid-dynamic response to a variety of external dynamic disturbances was evaluated for a spherical tank 137 cm in diameter. The evaluated cases included the tank ejection from the Shuttle payload bay, tank rotation about an axis of rotation outside of the tank, and axial accelerations. In all cases forces and moments applied to the tank by the fluid were calculated as were fluid-ullage interface configurations. A no-slip boundary condition at the tank sidewalls was assumed in all cases. A combination of nitrogen tetroxide (N_2O_4) and nitrogen dioxide (NO_2) in chemical equilibrium was the assumed fluid with the following properties: specific gravity, 2.83; surface tension, 26.5 dynes/cm ; viscosity, $0.4160 \text{ centipoise}$. A number of cases were considered, starting with the tank ejection from the Shuttle payload bay and proceeding through various orbital maneuvers.

Tank ejection from the Shuttle payload bay was conducted with a 20-percent ullage volume, assuming that the ullage volume is spherical in shape and can be located anywhere in the liquid bulk. Forces and moments for a number of bubble locations were then calculated, providing information on the vehicle motion during the ejection phase. Results have not been formally documented and are not reported here, since this is a rather mild case in a computational sense compared to the other cases. Results of analysis indicate that the vapor bubble usually stays intact until it approaches the tank surface, where a liquid jet frequently shoots through the bubble center line, breaking the bubble into a number of smaller ones.

Motion and acceleration histories for all cases considered are summarized in Table 1. All cases represent 20-percent loading level with

Table 1. Case Description

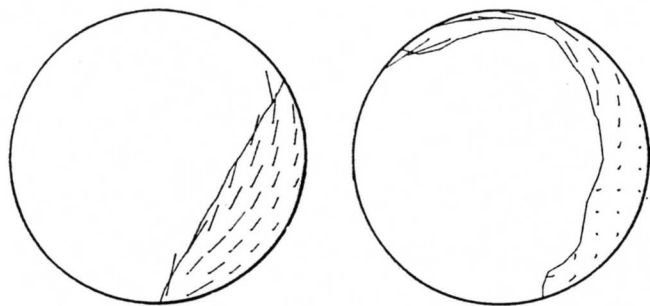
Case	Configuration	Duration (sec)	Acceleration History
1		45	 $a_r = 2.28 \text{ cm/sec}^2$ $a_z = 1.33 \text{ cm/sec}^2$
2		30	$a_z = 1.21 \text{ cm/sec}^2$
3		3.5	$a_z = 98.1 \text{ cm/sec}^2$, if time $< 2.5 \text{ sec}$ $a_z = 0$, if time $> 2.5 \text{ sec}$

initially flat liquid-vapor interface. Although a typical interface in a low-gravity field assumes a curved configuration, the degree of curvature depending on the contact angle and the gravity level, such a simplification would not significantly alter the results. A complicating factor in this type of analysis is a random initial-liquid location. Although only one initial liquid configuration is shown for each case, a number of other configurations were considered in order to determine which would yield the most critical results. The minimum acceleration level of 1.21 cm/sec^2 , representing Case 2, gives a Bond number of 311. The effect of surface tension, therefore, could be disregarded for all three cases.

Case 1 represents tank rotation about a point outside of the tank envelope, a case that would result from rotating a cluster of tanks about a common center of gravity. This case was considered to determine the forces and moments applied to the vehicle by fluid motion during and after a rotational orbital maneuver. The initial fluid angle was chosen to create a condition in which the liquid flows down both sides of the tank and eventually merges. This was done to check the code capability to track such motion and to create a condition with a severe dynamic disturbance. Cases 2 and 3 were considered to evaluate the effect of the settling acceleration level on the liquid settling characteristics and the resulting vehicle dynamic disturbances. Case 2 is rather similar in acceleration level to Case 1, although the acceleration is applied along one axis only, since no centrifugal acceleration is present. Case 3 represents a much greater settling acceleration level. The initial liquid angles of 3-deg and 1-deg, for Cases 2 and 3, respectively, were input to accelerate the initiation of liquid motion.

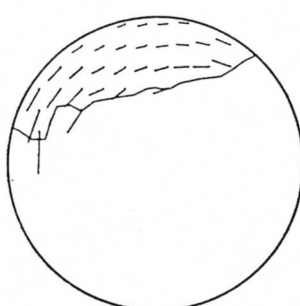
Case 1 liquid surface configuration and velocity vectors at four time frames are shown in Figure 2. The first frame shows liquid moving in one direction. This is caused by the initial predominance of tangential acceleration. As the centrifugal acceleration develops, part of the liquid reverses in velocity (second and third frames) with the two streams merging in the last frame. Vertical forces are shown in Figure 3. As shown by the results, there are no excessive forces either during or after the maneuver. The level of acceptable forces is established by specific system control requirements. In this particular case, no large globules separated from the liquid bulk, which could impact the opposite tank surface after the orientation maneuver, causing a significant disturbance when a stable platform is required.

Case 2 liquid motion is shown in Figure 4. Although the vertical acceleration level is similar to that of case 1, the resulting motion is quite different. In the first frame the liquid flows down the tank side, while in the second frame it begins to separate into two streams, and in the third is fully separated. The liquid configuration after the separated globule has impacted the liquid at the tank bottom is shown in the last frame. Perspective views of the liquid surface appear in Figure 5. Since



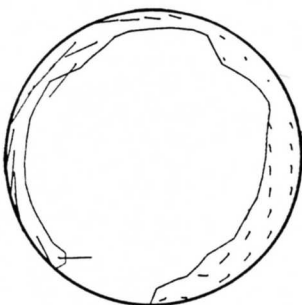
Time = 2.1 sec

Time = 23.7 sec

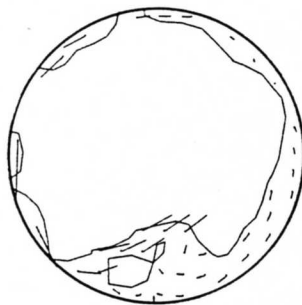


Time = 15.5 sec

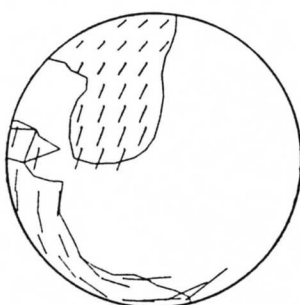
Time = 19.4 sec



Time = 38.7 sec



Time = 45.0 sec



Time = 25.3 sec



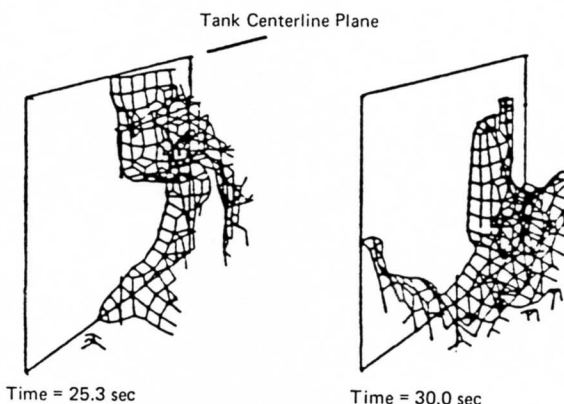
Time = 30.0 sec

Figure 2. Case 1 Fluid Configuration and Velocity Vectors

Figure 4. Case 2 Fluid Configuration and Velocity Vectors

the model was based on symmetry about a center plane, these contours are for one half of the tank. The first frame shows some liquid at the tank bottom with much of the remaining liquid approaching the tank bottom. The second frame shows the liquid configuration after the large liquid globule had impacted the liquid at the bottom of the tank. The vertical force history is shown in Figure 6. The large pressure peak at 29 seconds is quite obviously caused by the impact of the large globule. Although the total acceleration is much larger for Case 1 than Case 2, Case 2 results in larger maximum forces.

Case 3 liquid motion appears in Figure 7. Liquid separating into two streams is shown in the first frame. The second frame shows liquid globules separating from the middle stream, while the third frame shows most of the liquid settled at the tank bottom, with a column of liquid still approaching the tank bottom. The last frame shows liquid rebounding with a vertical velocity towards the upper surface. Vertical force history is given in Figure 8. The vertical force is shown to decrease as the liquid detaches from the upper surface. This persists up to 2.1 seconds. At 2.2 seconds the liquid mass at the left side of the tank



Time = 25.3 sec

Time = 30.0 sec

Figure 5. Case 2 Fluid Surface Configuration

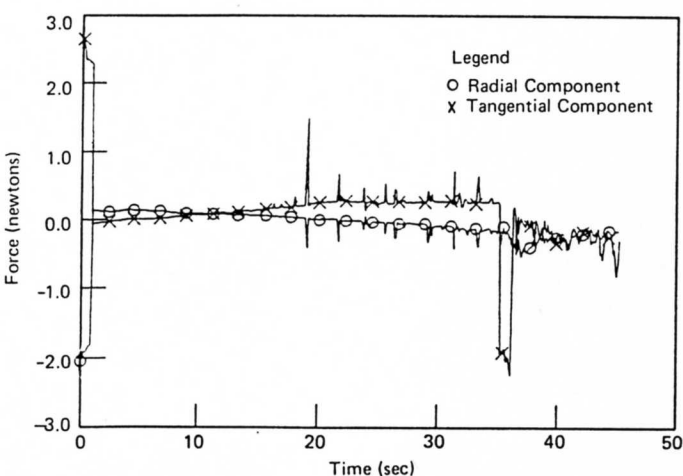


Figure 3. Case 1 Force Histories

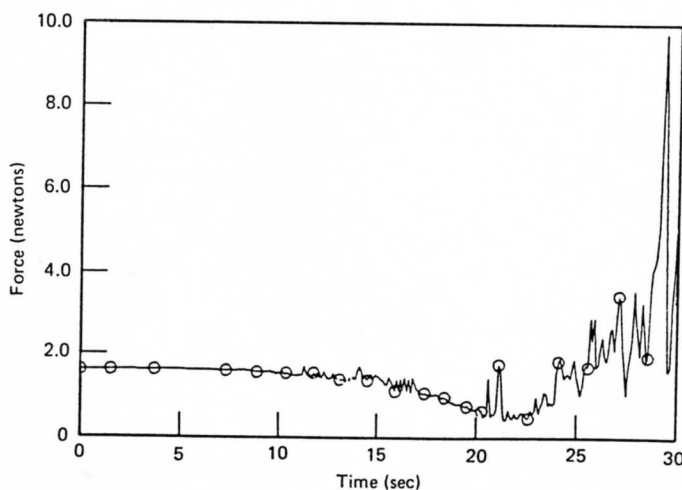


Figure 6. Case 2 Force History